Chemical Physics 19 (1977) 413–427

LONG RANGE EXCITON PERCOLATION AND SUPEREXCHANGE: ENERGY DENOMINATOR STUDY ON $^3B_{1u}$ NAPHTHALENE *

R. KOPELMAN, E.M. MONBERG and F.W. OCHS ‡
Department of Chemistry, The University of Michigan, Ann Arbor, Michigan 48109, USA

Received 22 October 1976

The long-range exciton percolation model is found to describe the lowest triplet exciton superexchange ("tunneling") migration at low temperature (2 K), in our model alloy system: Binary isotopic mixed naphthalene crystals with dispersed exciton sensors (supertraps) consisting of small concentrations of betamethylnaphthalene ($\sim 10^{-3}$ mole fraction) or isotopic substituted naphthalene molecules (with lower excitation energies than the partially deuterated naphthalene guest species). While the "host" is $C_{10}D_8$ throughout, the "guest" species in our five experimental systems are: $C_{10}H_8$, 2-$DC_{10}H_7$, 1-$DC_{10}H_7$, 1,4-$D_2C_{10}H_6$ and 1,4,5,8-$D_4C_{10}H_4$. The variation in guest–host (and supertrap–guest) energy denominator in the above systems enables a quantitative test of our physical exciton superechange (tunneling) migration model, in conjunction with a mathematical long-range percolation model (J. Hoshen, E.M. Monberg and R. Kopelman, unpublished). The experimental monitoring of the exciton migration dynamics consists of refined phosphorescence measurements on our systems, under highly controlled conditions (crystal quality, purity, concentration, temperature and excitation). Using only the known nearest neighbor (interchange-equivalent) exciton exchange interactions, quantitative agreement with the experimental dynamic percolation concentration is achieved, without adjustable parameters, for four of the five investigated systems. The fifth one is known to involve a cooperative percolation–thermalization exciton migration, and is effective in qualitative agreement with the predicted upper limit for the exciton percolation concentration. The nearest-neighbor $^3B_{1u}$ excitation exchange interactions, and their square lattice topology, play the dominant role in determining the guest triplet exciton energy transfer and migration. This energy conduction involves an extremely narrow "impurity band", on the order of 10 to 10^3 Hz, formed by the superexchange (tunneling) exciton interactions resulting from the above mentioned exciton exchange interactions (integrals). The latter are thus confirmed as the major contributors to the $^3B_{1u}$ exciton transfer, migration and energy band (3×10^{11} Hz) in the ordinary naphthalene crystal. Just below the percolation concentration the "impurity conduction band" further shrinks by one or two orders of magnitude, resulting in a bandwidth of about *one* hertz or less, and thus practically resulting in the "switching off" of the exciton transport. The tunneling radius is about 30 Å or larger, depending on the system, but essentially in the *ab* plane.

1. Introduction

The trap-to-trap migration concept was introduced [1] over a decade ago to describe long range triplet exciton transfer. It was suggested that such migration could occur by "tunneling" [1], i.e., a super-exchange type [2] interaction through the host exciton band, the direct Förster–Dexter type interaction [3] being of small importance for such long range (non-near neighbor) triplet exciton transfer. Recently [4], we have introduced the concept of exciton percolation which describes the onset of free exciton flow through the impurity and it was shown that, due to the increased trap-to-trap migration length in a long-lived triplet, the effective percolation for the triplet can occur at a much lower concentration than the static percolation [5] which defines the concentration at which the impurity density-of-states becomes a quasi-continuum.

To experimentally determine the exciton percolation concentration (which depends on the exciton life-time) for a given impurity (trap) a method was proposed [4] utilizing the doping of the sample with

* Supported by NSF Grant DMR75-07832 A01 and NIH Grant NS08116-08.
‡ Present address: Cal-Farm Insurance Co. 2855 Telegraph Avenue, Berkeley, California 94705.

a very small concentration of another trap of lower energy (supertrap) and using it to monitor the exciton flow. At the onset of the exciton percolation, the supertrap emission increases dramatically.

In this paper we present some studies on triplet energy transfer in multicomponent isotopic and chemical mixed naphthalene crystals. We find that as a supertrap is often "naturally" contained in the trap sample, the concentration of the trap and that of its supertrap are coupled and what one measures is an exciton percolation which explicitly depends on the concentration of the supertrap.

An energy denominator study of the exciton percolation reveals it to be highly dependent on the trap-depth, showing the importance of the indirect, i.e., superexchange interaction through the host exciton band. Using a superexchange approach, which is a modified Nieman and Robinson [1] formulation, for trap-to-trap ("virtual band") transfer we get good agreement with experiment without any adjustable parameters. To utilize the superexchange formalism we use a specially developed mathematical formalism of "long-range" percolation [6]. The long-range bond is defined as a succession of near-neighbor bonds. Using solely the known [7] interchange equivalent nearest-neighbor exciton interactions we get good agreement with experiment. Thus the important exciton exchange interaction of $^3B_{1u}$ naphthalene is confirmed to be in the *ab* plane and the superexchange interactions and transfer are largely two-dimensional. The "switching" (on-and-off) of the dynamical energy transfer of the lowest triplet exciton of naphthalene is found to depend, as expected [4], on the guest–host energy separation (denominator), on the guest concentration and on the supertrap concentration (relative to the guest). The superexchange interactions that dominate the energy transfer at the percolation point are sometimes as low as only a few hertz.

In the case of the α-D_4 $^{12}C_{10}H_4$ trap in the $C_{10}D_8$ host, we find that effective percolation occurs at a concentration much lower than would be expected from theoretical long-range percolation and superexchange considerations. We attribute this to cooperative percolation–thermalization, which will be discussed further in a future publication.

2. Experimental

Experiments were performed on chemical and isotopic mixed crystals with betamethylnaphthalene (BMN) and naphthalene $C_{10}H_8(H_8)$, 1-$DC_{10}H_7(\alpha D_1)$, 2-$DC_{10}H_7(\beta D_1)$, 1,4-$D_2C_{10}H_6(\alpha D_2)$, 1,4,5,8-$D_4C_{10}H_4(\alpha D_4)$ as guests in $C_{10}D_8(D_8)$ as the host. The D_8 (Merck, Sharp and Dohme; International Chemical and Nuclear Corp.; Thompson Packard Inc.; 99.0% deuterium atom purity) was first zone refined (50 passes) then potassium treated to reduce the concentration of interfering β-methylnaphthalene (even in the cases where it was later added), and finally extensively zone refined (>200 passes). The partially deuterated naphthalenes obtained from Merck, Sharp and Dohme were purified only by zone refining (several hundred passes), as it has been demonstrated [8] that during the potassium treatment protons and deuterons are exchanged. The purity of these compounds was determined mainly by mass spectra and NMR, the latter being used to determine the actual position (α or β) of the proton positions in the partially deuterated compounds. Table 1 summarizes the isotopic purity of the compounds used in the various crystals [9]. The actual concentrations of the guest ($C_{10}H_8$) species in the $C_{10}H_8/C_{10}D_8$/BMN crystals was determined by mass spectrometry and the BMN concentration was found by gas–liquid chromatography. It should be mentioned that BMN seemed to be soluble in naphthalene only up to a concentration of ~0.1%. Above this concentration it began to form micro-crystals of BMN as it was excluded to the outer surface of the boule. We also carried out spectroscopic absorption experiments (at 2 K and 77 K) to check the relative concentrations of the components, as well as NMR experiments [9] (see table 1).

The crystals were grown from the melt, cleaved along the cleavage plane (*ab*) and mounted in a crystal holder which was in the form of a metal frame cage so that the crystal could move freely within the holder. Thus the crystal was subject to minimal strain. The crystals were always checked to be optically single by observation through crossed polarizers. Also, X-ray precession photographs were taken to determine the alignment of most of the crystals.

Table 1
Isotopic purity of isotopically substituted naphthalenes

$C_{10}D_8$

Species	% Abundance c)				
	ICN 20696 a)	TP 1 b)	TP 2	TP3	TP 4
$C_{10}D_8$	95.2	92.5	91.3	92.1	92.7
$C_{10}D_7H$	4.9	6.7	8.7	7.5	7.2
$C_{10}D_6H_2$		0.8		0.4	0.1
$C_{10}H_8$					0.008
Total deuteration	99.4±0.1%	99.0±0.1%	98.9±0.1%	99.1±0.1%	99.0±0.1%

$1,4,5,8\text{-}D_4C_{10}H_4(\alpha D_4)$

Species	% Abundance c)
$C_{10}D_6H_2$	1.5
$C_{10}D_5H_3$	11.4
$C_{10}D_4H_4$	73.4
$C_{10}D_3H_5$	9.5
$C_{10}D_2H_6$	3.3
$C_{10}DH_7$	0.9

NMR indicates that the fraction of α protons present is < 0.05 indicating that the α positions are highly more deuterated than the β positions [9].

$1,4\text{-}D_2C_{10}H_6(\alpha D_2)$ [Merck, Sharp, Dohme]

Species	% Abundance c)
$C_{10}H_6D_2$	98.0
$C_{10}H_7D$	1.8
$C_{10}H_8$	0.1

The integrated intensity of α proton NMR divided by the β proton intensity [9] is 0.43 ± 0.05. The expected ratio is 0.5 for pure α substituted D_2.

$2\text{-}DC_{10}H_7(\beta D_1)$ [Merck, Sharp, Dohme]

Species	% Abundance c)
$C_{10}H_6D_2$	0.14
$C_{10}H_7D$	97.1
$C_{10}H_8$	2.64

Ratio of α to β protons from NMR is 1.7. The expected ratio is 1.33 for pure $2\text{-}DC_{10}H_7$.

$1\text{-}DC_{10}H_7(\alpha D_1)$

Species	% Abundance c)
$C_{10}H_6D_2$	0.51
$C_{10}H_7D$	97.3
$C_{10}H_8$	2.18

Ratio of α to β protons from NMR spectrum is 0.78; 0.75 is *expected* for pure $1\text{-}D_1$.

a) International Chemical and Nuclear Corp. Lot number 20696. b) Thompson-Packard.
c) Mass spectral data corrected for ^{13}C contributions.
Notes: (1) The relative isotopic naphthalene concentrations are confirmed by absorption spectra (see refs. [9] and [10]).
(2) The concentrations of BMN in our chemically mixed crystals are given for each sample in ref. [28], as well as detailed analytical procedures.

The crystal was immersed in supercooled liquid helium with a temperature of 1.6–2.0 K (determined by measuring the pressure of helium gas above the liquid). A 1600 watt Hanovia Xenon lamp was used as a light source. For calibration, a Westinghouse iron-neon hollow cathode was used. When phosphorescence spectra were recorded, the filter consisted of a solution of 170 g/ℓ of $NiSO_4$ and 40 g/ℓ $CoSO_4$ with a 5 cm pathlength and either a Corning CS7-54 or a Schott UG-11 glass filter. Also a Corning CS0-52 glass filter was used at the spectrometer slit to prevent the second order fluorescence overlap. The lamp was set at a right angle to the spectrometer axis so that the front surface of the crystal was illuminated and reabsorbtion of the origin was minimized.

The spectra were recorded photoelectrically on a Jarrel-Ash model 25-100, 1 meter, double Czerny-Turner spectrograph–spectrometer. The detection system consisted of an ITT F4013 photomultiplier mounted in a Products for Research housing cooled to below −10°C. The signal from the photomultiplier was fed to an SSR Instruments model 1120 discriminator/amplifier which was in turn connected to an SSR Instruments model 1110 digital synchronous computer. The output of the latter was interfaced with a Kennedy 9-track magnetic tape. A mirrored

chopper (Princeton Applied Research chopper motor and Brower Laboratory mirrored chopper blade) allowed the simultaneous recording of both the crystal spectrum and the calibration spectrum. A calibrated plot was obtained from the data recorded on magnetic tape with the aid of specially designed [9] software and an IBM 360/67 (or Amdahl 470V/6) computer. Another computer program [9] provides for versatile plotting options, objective despiking and smoothing, as well as "interaction" with the spectrum on a graphics terminal, adding spectra together and integrating peak intensities while subtracting background.

3. Experimental results

Fig. 1 shows a concentration dependence study of the 2 K phosphorescence in the origin region of the added guest naphthalene-αD_4 (unless otherwise indicated this nomenclature implies all $\alpha D_4{}^{13}C_n{}^{12}C_{10-n}H_4$ isomers, with the prefix indicating the position of the deuterium substitution, and the same convention will be used for other partially substituted isotopic naphthalenes). The host is always naphthalene-D_8. Spectrum A is obtained from the crystal containing 0.039% mole of the αD_4 sample (which also contains αD_3, αD_2, αD_1, H_8, etc.). The strongest peak (21271 cm^{-1}) in the spectrum belongs to αD_4. The other two major peaks (21256, 21240 cm^{-1}), correspond to αD_3 and αD_2. The triplet origin assignment for the various naphthalenes in naphthalene-D_8 host has already been presented elsewhere [10]. The peak (21279 cm^{-1}) corresponding to the D_5 origin can also be seen. It should be noted that the αD_4 peak has an asymmetry on the high energy side. Spectrum B has been obtained from a crystal containing 0.35% mole of αD_4 in the D_8 host. Several changes have taken place in going from the 0.039% to the 0.35% sample. The intensity of αD_4 has decreased considerably, while that of αD_2 has been greatly enhanced. On the other hand, there is no significant change in the αD_3 intensity. This shows a selective large energy transfer between αD_4 and αD_2 even at this low concentration. The peak corresponding to D_5 can barely be seen above the noise level. Furthermore, the peak due to αD_4 has an asymmetry appearing now on the lower energy side. Comparing the αD_4 bands in these

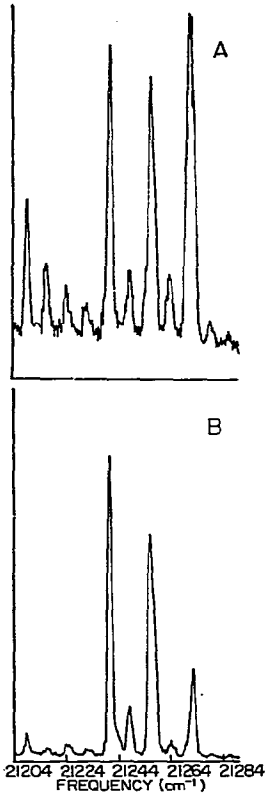

Fig. 1. Concentration dependence of 1,4,5,8-$D_4C_{10}H_4$ in $C_{10}D_8$ phosphorescence. In A the total guest concentration (see table 1) is 0.039% mole while in B it is 0.35% mole. The resolution of both of these photoelectrically (photon counting) recorded spectra is 1 cm^{-1}.

crystals of two different αD_4 concentrations, we find that the peak in the higher concentration (0.35%) is *shifted* about 1.5 cm^{-1} to higher energy, relative to the peak in the 0.039% crystal. This shift corresponds to the one observed for ^{13}C substitution for the naphthalene triplet state [9,11]. On this basis we feel that in the 0.039% crystal spectrum the major peak corresponds to $\alpha D_4{}^{12}C_{10}H_4$, the higher energy asymmetry being due to the unresolved $\alpha D_4{}^{13}C^{12}C_9H_4$ peak. On the other hand, in the 0.35% sample, the peak

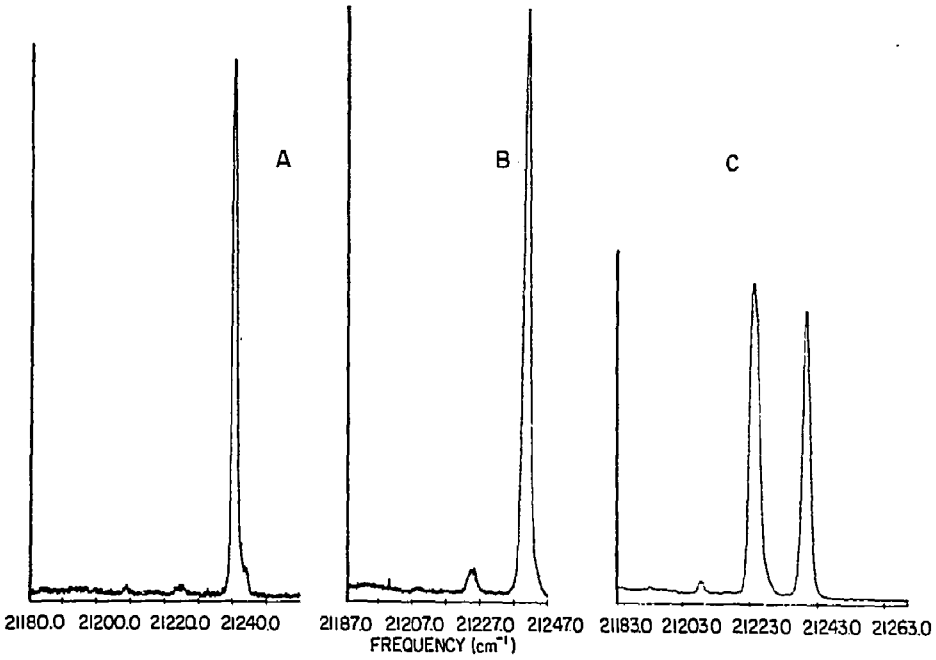

Fig. 2. Concentration dependence of the 1,4-$D_2C_{10}H_6$ in $C_{10}D_8$ phosphorescence spectrum. The higher energy peak in all three spectra is the 1,4-D_2 peak. The next lower in energy is 1-D_1 and the weak feature at lowest energy is $C_{10}H_8$. In spectrum A the concentration of guest was 0.22% mole; in B, 1%; and in C, 5.1%. The 0.07% mole spectrum was omitted but is identical to A. The resolution was 1 cm^{-1} in all of these spectra and the spectra were recorded photoelectrically. The relative concentrations of other guests is indicated in table 1.

is due to $\alpha D_4{}^{13}C^{12}C_9H_4$ while the asymmetry on the lower energy side is due to $\alpha D_4{}^{12}C_{10}H_4$. This implies that only $\alpha D_4{}^{12}C_{10}H_4$ and not $\alpha D_4{}^{13}C^{12}C_9H_4$ has transferred its energy to its supertraps.

Fig. 2 exhibits the phosphorescence from crystals containing different concentrations of αD_2 in the D_8 host. Here αD_2 is the trap while αD_1 and H_8 are the principal supertraps. As the concentration of αD_2 increases the intensity shifts from αD_2 to αD_1 and H_8. However, the concentration at which the relative intensity of the trap and the supertrap switches is now much higher (5%).

Figs. 3 and 4 show similar studies on crystals composed of different concentrations, respectively, of αD_1 and βD_1 in the D_8 host. For the former the supertraps are βD_1 and H_8, while the latter has only one supertrap, H_8. Here, again, with increasing trap concentration the intensity of the peaks of the supertraps grow while that of the traps decreases. Once again, in the case of αD_1 where there are two supertraps (βD_1 and H_8) αD_1 appears to transfer energy selectively to one supertrap, H_8.

In fig. 5 we see the phosphorescence from several crystals containing increasing amounts of $C_{10}H_8$ while the BMN concentration is held constant at a level of less than 0.001. Here $C_{10}H_8$ is the trap and BMN is the supertrap. As the concentration of $C_{10}H_8$ increases, the emission intensity shifts from $C_{10}H_8$ to BMN. The guest concentration at which the above mentioned intensity shift occurs is now about 9%. Note also the $C_{10}H_8$ linebroadening just above percolation (not yet observed even at 8.3%). Fig. 6 demonstrates this shift and its catastrophic nature. Here the abscissa C_G is the total concentration of guests (including trap and supertrap, for theoretical reasons [4]), while the ordinate is I_S/I_{total} for reasons discussed below. However, we note here that the omission of the relative molar cross section $\bar{\gamma}$ (including both radiative yields and trapping efficiencies – see below), makes little difference in the major features of the curve (fig. 6).

In summarizing the results obtained, we see that in

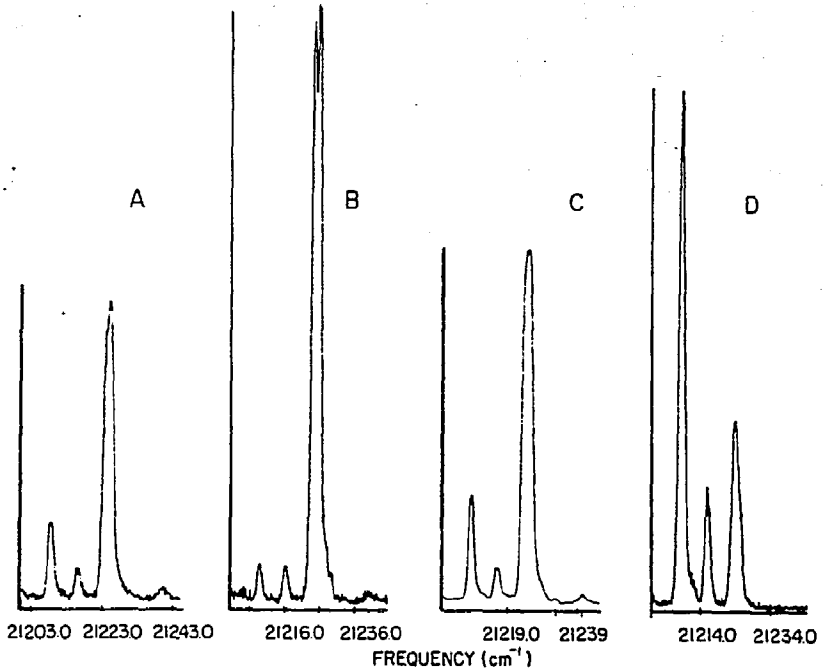

Fig. 3. Concentration dependence of the phosphorescence spectrum of 1-$D_1C_{10}H_7$ in $C_{10}D_8$. The concentrations of guests for spectra A to D are 0.088% mole, 0.22% mole, 0.7% mole and 5.0% mole, respectively. The relative concentrations of impurities in the 1-D_1 are indicated in table 1 (in fig. B the orientation splitting can be observed). All four spectra were recorded photoelectrically with a 1 cm^{-1} resolution, except B which has a resolution of about 0.7 cm^{-1}.

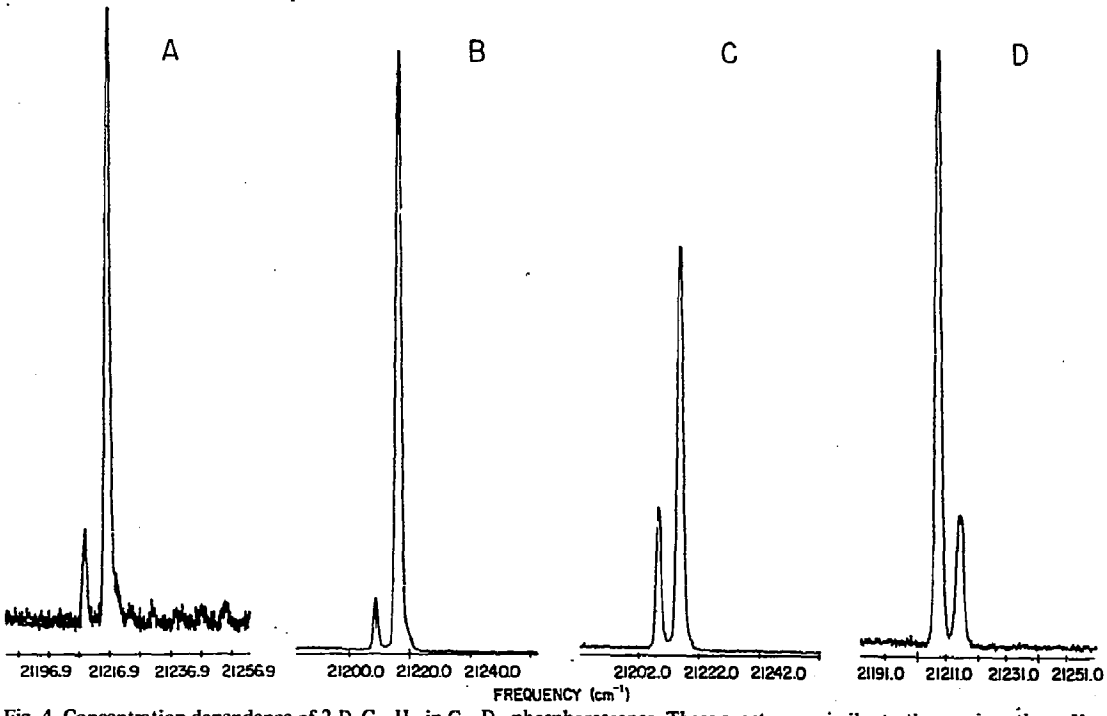

Fig. 4. Concentration dependence of 2-$D_1C_{10}H_7$ in $C_{10}D_8$ phosphorescence. These spectra are similar to the previous three. Here the principal guest is 2-D_1 (concentrations of other guests, relative to 2-D_1, are indicated in table 1) in concentration of 0.009% mole, 0.91% mole, 4.9% mole, and 10% mole from A to D.

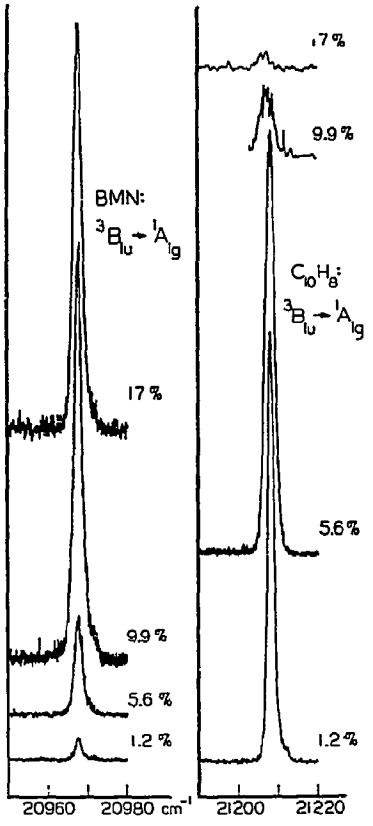

Fig. 5. Concentration dependence of the trap ($C_{10}H_8$) and supertrap (BMN) phosphorescence in a $C_{10}D_8$ host at 1.7 K. The concentrations are given in mole percent guest ($C_{10}H_8$), while the BMN (betamethylnaphthalene) concentration is roughly constant (~0.1%). The relative intensities (photon counts) are quantitative only for transitions at the same guest concentration. Note the broadening of the $C_{10}H_8$ peak above the precolation concentration. The exact BMN concentrations are given in ref. [28].

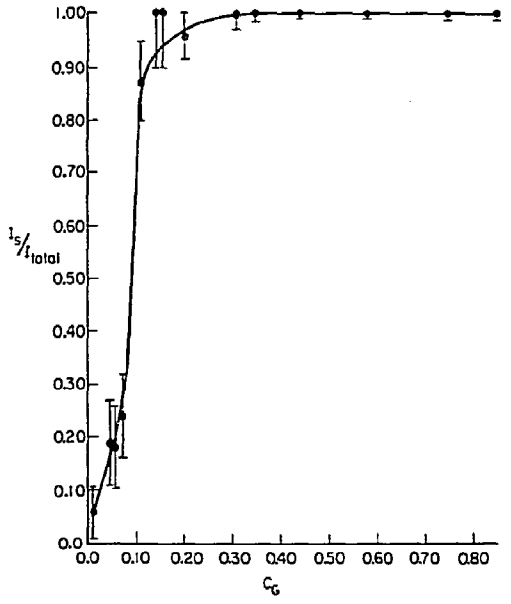

Fig. 6. Experimental percolation curve for $C_{10}H_8$ (trap) in $C_{10}D_8$ (host) with a BMN sensor (supertrap) at 1.7 K. I_S/I_{total} is the ratio of the integrated intensities, sensor to total guest, where "total guest" refers to the sum of trap and supertrap integrated intensities. C_G is the total guest concentration (mole fraction), which is practically the same as the trap concentration, the supertrap concentration being about 10^{-3} mole fraction throughout. The points are derived by integration of spectra, some of which have been shown in fig. 5. The exact concentrations and cluster compositions for each data point are tabulated in ref. [28].

the multicomponent systems investigated, as the concentration of the trap increases the intensity shifts to a supertrap. However, the concentration at which the shift in relative intensity, from the trap to its supertrap, occurs is dependent on the trapdepth, increasing with an increase in the trapdepth. The energy transfer from a particular trap to its supertraps also appears to be selective [9]. The first effect is discussed quantitatively below while the second one, partially discussed in [9], will be discussed further elsewhere.

4. Some definitions

The molecules with highest excitation energy form the *host*, by definition, irrespective of its concentration. Generally, the "host" is the majority component, but it may include some impurity components of similar energy, usually differing only by the isotopic composition of one or two atoms (carbon or hydrogen).

The molecules with significantly lower energy (relative to kT) than that of the host form the *traps* and *supertraps*. The highest energy *trap* is usually called the *guest*. It is usually present in higher concentrations than the still lower energy traps. The latter are called *supertraps*. However, the "guest" may include some "impurity" traps, which are very close to it in energy, usually differing from it only by the iso-

topic composition of one or two of its atoms (carbons only).

While there usually exist more than one *supertrap* species, we deal with all these species collectively as "supertraps". Also, *total guest* means traps and supertraps *combined*.

The *effective percolation concentration* is defined here to be the turning point in the ratio of *combined supertrap emission/trap emission*, i.e., when this ratio becomes unity.

5. Synopsis of experimental results

The systems discussed are tabulated (table 2). For systems I–IV the relation

$$\Delta \equiv E_h - E_g \gg kT \qquad (1)$$

is well obeyed at our temperature of investigation (2 K), where h designates the *host* and g the *guest* (trap) species. However, this relation (eq. 1) is not good enough for system V, which will be discussed, therefore, separately (see also ref. [9]).

A series of emission spectra was shown (fig. 5) for system I (see table 2). These are summarized in fig. 6. It can easily be seen that the effective percolation concentration is at about 0.09 ± 0.02 mole fraction of guest.

The behaviour of system II (see table 2) is demonstrated by its series of emission spectra (fig. 4). It can easily be seen that the effective percolation concentration is about 0.07 ± 0.02 mole fraction guest. Similarly, the behaviour of system III (see table 2) is demonstrated by its emission spectra (fig. 3). Its effective guest percolation concentration is 0.03 ± 0.02 mole fraction. The system IV (table 1) behaviour is given in fig. 2. Its effective guest percolation concentration is 0.04 ± 0.01 mole fraction.

System V "percolates" at a concentration of about 10^{-3} (fig. 1). As eq. (1) is not quite justified for it, this case will be discussed in a separate paper, together with the higher temperature results of systems I–IV.

6. Percolation and superexchange

Site percolation [12,13], for a given topology, merely depends on the range of interactions. While most ordinary examples of lattice site percolation assume nearest neighbor only interactions, longer range interactions have been considered [6]. For instance, for an infinite *square* lattice the critical (percolation) concentration [12] is 0.59, implying nearest neighbor only interactions. However, by adding next-nearest neighbors, this value gets reduced to 0.41 for what is generally called [12] *square (1,2)*. This process can be generalized to next-next-nearest-neighbor interactions [6], giving the *square (1,2,3)* lattice with $C_c = 0.29$, etc.

If one considers a guest–host–guest type interaction (tunneling or superexchange) [4,5] then it is of interest to count the number of intervening "bonds" [6]. For instance, *one* intervening host site means 2 bonds between the two guest sites, *two* intervening host sites means 3 bonds, three intervening host sites means 4 intervening bonds, etc. We notice that allowing *one* intervening host site (i.e., 2 bonds) in a square lattice, and counting over both one bond and two

Table 2
List of experimental systems

System	Host	Guest (trap)	$E_h - E_g$ (cm^{-1})	Supertraps (major)
I	$C_{10}D_8$	$C_{10}H_8$	88 a)	BMN b)
II	$C_{10}D_8$	$2\text{-}DC_{10}H_7$	81 a)	$C_{10}H_8$
III	$C_{10}D_8$	$1\text{-}DC_{10}H_7$	72 a)	$2\text{-}DC_{10}H_7$; $C_{10}H_8$
IV	$C_{10}D_8$	$1,4\text{-}D_2C_{10}H_6$	57 a)	$1\text{-}DC_{10}H_7$; $C_{10}H_8$
V	$C_{10}D_8$	$1,4,5,8\text{-}D_4C_{10}H_4$	27 a)	$1,4,5\text{-}D_3C_{10}H_5$; $1,4\text{-}D_2C_{10}H_6$

a) The difference between the host excitation energy (E_h) and guest energy (E_g) assumes a pure host (E_h is the bottom of the exciton band) and a highly dilute guest (E_g is isolated monomer energy). See ref. [10].

b) BMN is betamethylnaphthalene.

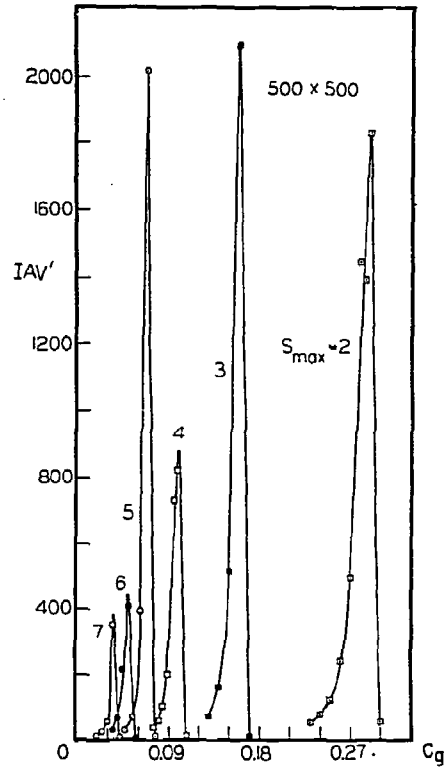

Fig. 7. Long range percolation for a square lattice. $S_{max}(\equiv n)$ is the number of successive nearest-neighbor bonds. I'_{AV} is the reduced average cluster size [6,15]. The discontinuity in the I'_{AV} vs the molar guest concentration (C_G) curve gives the critical percolation concentration [4,12]. The data are taken from ref. [6] and were derived for a 500 X 500 lattice. Only the relative, but not the absolute, ordinate values are significant (due to statistical fluctuations) [6]. Results [6] for $S_{max} > 7$ are not shown here but are given by [6]: $C_c(S_{max}) = 4(2S^2_{max} + 2S_{max} + 1)^{-1}$.

bond interactions results in the *square (1,2,3)* topology, *not* the *square (1,2)*. We have investigated [6] the site percolation problem for square lattices up to "twelve bond" interactions ($S_{max} = 12$). The results are shown in fig. 7 (up to $S_{max} = 7$).

For the specific problem of interest, the lowest triplet exciton of naphthalene, we consider only the nearest neighbor exciton interaction [13], i.e., the $\pm\frac{1}{2}(\boldsymbol{a} \pm \boldsymbol{b})$ interactions, where $\boldsymbol{b}$ is the monoclinic axis [14]. With this limitation, we consider only a two-dimensional lattice (the $\boldsymbol{a}$-$\boldsymbol{b}$ plane) with a topology equivalent to that of the square lattice. Thus, to find the critical percolation concentration, the only remaining problem is the superexchange interaction range, i.e., the value of S_{max}.

The superexchange interaction in such a square lattice ($M_{0,n}$) is given [9] by

$$M_{0,n} = \Gamma_n \beta^n / \Delta^{n-1}, \qquad \text{iff } \beta \ll \Delta, \tag{2}$$

where the second guest is n bonds away from the one at the origin (0), i.e., there are $(n-1)$ intervening host sites. Here β is the nearest neighbor pairwise interaction, Δ the trapdepth (guest–host energy separation in the ideal mixed crystal [2]) and Γ_n a geometrical factor, given by the number of paths, involving n bonds, between the two guest sites. The minimum value of Γ_n is *one*, in the case where all n bonds are on a straight line. The maximum value ($\Gamma^{\backslash}_n$) is found for the zig-zag path, i.e., when the number of "zigs" equals the number of "zags". In the latter case [9]:

$$\Gamma^{\backslash}_n = n!/[(n/2)!]^2$$
$$\text{iff } n = \text{even, zig-zag path,} \tag{3a}$$

$$\Gamma^{\backslash}_n = n!/\{[(n-1)/2]!\,[(n+1)/2]!\}$$
$$\text{iff } n = \text{odd, zig-zag path.} \tag{3b}$$

For intermediate paths, i.e., paths including more "zigs" than "zags", one has intermediate values. Thus one gets for the general case of the geometric factor:

$$1 \leqslant \Gamma_n \leqslant \Gamma^{\backslash}_n . \tag{4}$$

Finally, to find the effective maximum range $\bar{n}$ of the interaction, the total average *time* of exciton transfer has to be considered [4]. We thus argue that for "effective percolation" to happen, there has to be an even probability of the exciton *registering on a sensor* [15], i.e., emitting from the supertrap. The relative probability of supertrap registration [15], *without* energy transfer (normalized to $\bar{\gamma} = 1$, see below) is

$$P = \bar{C}_S \equiv C_S / C_G , \tag{5}$$

where C_S is the supertrap concentration and C_G the guest (total) concentration (in mole fraction). In our present experiment this is less than 0.1 and will be practically neglected (though clearly visible on our low-guest-concentration spectra). In order to attain a probability of 0.5, the exciton transfer has to be efficient enough so as to result in roughly a 50:50 chance for registering on the sensor. Thus the exciton has to visit, within its lifetime, m distinct sites (not counting

the host sites tunnelled through), where

$$m \approx \bar{C}_S^{-1}\gamma^{-1}, \tag{6}$$

and γ is the trapping efficiency of the supertrap [15]. Assuming *random walk*, the exciton has to perform $\bar{m}$ hops (steps), where $\bar{m} \gtrsim m$, and [16–18]

$$m \approx \pi\bar{m}/\log \bar{m} \qquad (\text{iff } m \gg 1). \tag{7}$$

Out of the $\bar{m}$ hops, $\bar{m}^{\backslash}$ involve the largest path (length $\bar{n}$) [19]. Below the percolation concentration, paths of $n < \bar{n}$ are rare [20], so that $\bar{m}^{\backslash}$ is close to $\bar{m}$:

$$\bar{m} \gtrsim \bar{m}^{\backslash}. \tag{8}$$

We thus *assume* that (roughly):

$$\bar{m}^{\backslash} \approx m. \tag{9}$$

The time it takes [21] for one guest–guest hop is:

$$t_{0,n} \approx (4M_{0,n})^{-1}, \tag{10}$$

where $t_{0,n}$ is in seconds and M in units of hertz. We assume that a guest–supertrap hop takes roughly the same time as a trap–trap hop (this assumption is not crucial as guest–supertrap hops are rare, with a rough probability of $\bar{C}_S^{-1}$). We also note that the relatively rare hops of $n < \bar{n}$ have a much shorter hopping time:

$$t_{0,n} \ll t_{0,\bar{n}}, \qquad \text{iff } n < \bar{n}.$$

We can thus write a *total time* of transfer (t), neglecting also [20,22] the very rare hops of $n > \bar{n}$,

$$t = \sum_{i=1}^{\bar{m}^{\backslash}} (t_{0,\bar{n}})_i. \tag{11}$$

Now the different $(t_{0,\bar{n}})_i$ differ only due to a variation in $\Gamma_{\bar{n}}$, as $\beta^{\bar{n}}$ and $\Delta^{\bar{n}-1}$ are fixed for a given crystal. If we use an *average* $\bar{\Gamma}_{\bar{n}}$, i.e.,

$$\bar{\Gamma}_{\bar{n}} \equiv (1 + \Gamma_{\bar{n}}^{\backslash})/2 \approx \Gamma_{\bar{n}}^{\backslash}/2 \tag{12}$$

one can write:

$$t = \bar{m}^{\backslash}\bar{t}_{0,\bar{n}}, \tag{13}$$

where

$$\bar{t}_{0,n} = (4\bar{M}_{0,\bar{n}})^{-1} \tag{14}$$

and

$$\bar{M}_{0,\bar{n}} = \bar{\Gamma}_{\bar{n}}\beta^{\bar{n}}/\Delta^{\bar{n}-1}. \tag{15}$$

Therefore, from eqs. (6, 9, 10, 13–15):

$$t \approx m\bar{t}_{0,\bar{n}} \approx \bar{C}_S^{-1}\gamma^{-1}\bar{t}_{0,\bar{n}} \tag{16}$$

$$= \bar{C}_S^{-1}\gamma^{-1}(4\bar{M}_{0,\bar{n}})^{-1} \tag{16a}$$

$$= \Delta^{\bar{n}-1}/(4\bar{C}_S\gamma\bar{\Gamma}_{\bar{n}}\beta^{\bar{n}}). \tag{16b}$$

This total transfer time is close to the guest exciton lifetime (half-life) τ_g, but a bit smaller, as we neglected, timewise, hops of $n \neq \bar{n}$, so that

$$t \lesssim \tau_g. \tag{17}$$

We can thus write

$$\Delta^{\bar{n}-1}/(4\bar{C}_S\gamma\bar{\Gamma}_{\bar{n}}\beta^{\bar{n}}) \lesssim \tau_g. \tag{18}$$

This equation can be utilized in one of two ways. The first is to assume a trapping efficiency γ (say $\gamma = 0.5$), calculate $\bar{n}$ (an integer!) and predict the effective percolation concentration (using fig. 7), to be compared with experiment. In the second alternative, we fit γ to the experiment. We note that, in our series of systems, we may expect γ to be roughly constant, at least in the isotopic series (II–V), unless it is quite sensitive to the trap–supertrap energy difference $(E_g - E_s)$, i.e., because of phonon Franck–Condon factors [23,9].

Finally, we note that ideally the supertrap is a *deep trap*:

$$\Delta' = E_g - E_s \gg kT. \tag{19}$$

However, this relationship is strictly true only for system I. Thus even for the case of perfect energy transfer, leading to complete equilibrium among the excitations, we expect non-negligible guest (trap) emission:

$$I_t/I_S = (C_t/C_S)\exp(-\Delta'/kT),$$

$$C_t \equiv C_G - C_S \approx C_G, \tag{20}$$

where we have assumed equal radiative yields of trap (t) and supertrap, and also Boltzmann equilibrium (among the excited states). Thus for C_G much above percolation we get:

$$I_S/(I_S + I_t) \approx \{1 + [\bar{C}_S \exp(\Delta'/kT)]^{-1}\}^{-1}, \tag{21}$$

for $C_G \gg C_c$.

7. Relative radiative yields and trapping efficiency

For C_G much below percolation, the emissions of

trap and supertrap are determined by their relative cross sections of host exciton trapping (and direct excitation), which are roughly proportional to their concentrations:

$$I_S/(I_S+I_t) \approx I_S/I_t \approx \bar{\gamma}\bar{C}_S, \quad \text{for } C_S \ll C_G \ll C_c, \quad (22)$$

where $\bar{\gamma}$ is a relative molar cross section, for *host* trapping efficiency, but normalized for radiative yields of sensor and trap. $\bar{\gamma}$ is of the order of unity [24], as both the ratios of sensor to trap radiative yields (for the 0–0 phosphorescence) and host trapping efficiencies are roughly unity [24], as is evident from the following discussion.

In ref. [28] we used as a measure of energy migration the expression:

$$P = I_S/(I_S + \alpha I_t) \equiv I_S/I_{total}. \quad (22a)$$

The expression I_S/I_{total} used as ordinate in fig. 6 implies $I_{total} \equiv I_S + I_t$, as we did not correct for α, which is similar to the inverse of $\bar{\gamma}$. Noting the similar value of I_S/I_{total} in fig. 6 and in the singlet exciton case of the same system (table 1 of ref. [28]), for the lowest C_G sample (1.2%) where no trap-to-supertrap energy transfer is likely in either system, we conclude that α is close to that in the singlet system [28], i.e., $\alpha = 2$. Assuming that most of the direct host (to-trap or to-supertrap) energy trapping occurs in the singlet system, we get [28] for the relative trapping efficiency about unity (compare ref. [24]) and for the relative radiative yields (BMN/$C_{10}H_8$) the value 2. Obviously, for traps and supertraps differing only by isotopic substitution, we expect the relative radiative yields to be close to unity. As mentioned, a ratio of unity is less obvious for the relative trapping efficiencies [9] (see also below), but is still implied here to be roughly correct.

8. Discussion

First, it will be shown that the energy transfer does take place in the triplet state, as opposed to energy transfer in the singlet state followed by intramolecular intersystem-crossing, even though the excitation originates in the singlet manifold. The singlet state of βD_1 is above that of the αD_1, while in the triplet state the energy levels of the two are switched [9]. Thus, if the energy transfer had taken place in the singlet, followed by fast intramolecular intersystem-crossing, we would not have seen any triplet emission from βD_1 in the sample prepared with βD_1 (which contains αD_1 impurity) in the D_8 host. On the other hand, we do see emission from βD_1 (and practically none from αD_1) which suggests that the energy transfer is taking place in the triplet (this does not preclude energy transfer in both manifolds, involving intermolecular guest–host intersystem-crossing). Also, the crystal containing 0.35% αD_4 has the relative fluorescence intensities of αD_4, αD_3 and αD_2 about the same as their absorptions [9].

We have seen that the concentration at which the intensity shift between a trap and a supertrap takes place, indicating substantive energy transfer, is dependent on the trapdepth. This clearly establishes the importance of the indirect, superexchange interaction (trap-to-trap migration) for the energy transfer, as opposed to a direct, Forster type interaction [3].

Due to the finite lifetime of the triplet state, the excitation can move by trap-to-trap migration only through a certain number of trap sites. The separation between trap sites we call the *tunnel length*. As pointed out before, the effective tunnel length here is about 6 to 7 nearest neighbor bonds in succession (see table 3), and is closely related to the tunneling (or hop) time t (eq. 10). Also related is the tunneling (superexchange) energy interaction (eq. 2). With the values of table 3 it can easily be seen that $M_{0,n}$ is only of the order of 10 to 10^3 hertz, compared to exchange interactions of the order of 1 cm^{-1} (3×10^{10} hertz). At percolation this gives impurity (virtual [1]) exciton conduction bandwidths of 10 to 10^3 hertz.

Table 3 gives a comparison of the experimental and theoretical critical percolation concentrations, based on eq. (18). The approach is to assume first a constant trapping efficiency $\gamma = 0.5$ (this is an absolute value, unlike that discussed above) and then to find the maximum $\bar{n}$ obeying eq. (18). The value of this $\bar{n}$ and the related $\Gamma_{\bar{n}}$ and t are in italics in the table, as well as the corresponding $C_G(\bar{n})$ taken from fig. 7 (except for system V, for reasons given below). We assumed a relatively high γ, based on phonon amalgamation [15].

The striking result in table 3 is the close agreement of the *experimental* C_G(percol.) and the theoretical $C_G(\bar{n})$. Also, it can be seen from the t-column of table 3 that the exciton transfer time t, based on eq.

Table 3
Comparison of experimental and theoretical percolation concentrations (based on eq. (18), with $\beta = 1.25\ cm^{-1}$)

System	C_G(percol.) (mole fraction)	$\bar{C}_S$	γ	Δ (cm^{-1})	$\bar{n}$	$\Gamma_{\bar{n}}$	t (s)	τ_g (s)	$C_G(\bar{n})$ (mole fraction)
I	0.09 ± 0.02	0.01	0.5	93	6	10	4.4	2.6 [a]	0.05
			0.5		*5*	*5*	*6.4×10^{-2}*	2.5 [b]	*0.07*
			0.05		4	3.5	$\sim 6 \times 10^{-2}$		0.10
II	0.07 ± 0.02	0.03	0.5	86	7	18	3.0	2.8 [c]	0.035
					6	*10*	*6.9×10^{-2}*	2.6 [b]	*0.05*
III	0.03 ± 0.02	0.09	0.5	77	*7*	*18*	*0.90*	3.0 [c]	*0.035*
					6	10	2.1×10^{-2}		0.05
IV	0.04 ± 0.01	0.04	0.5	62	*7*	*18*	*1.6*	3.65 [d]	*0.035*
					6	10	3.8×10^{-2}		0.05
V	10^{-3}	0.10	0.5	32	10	126	5.0	5.4 [b]	(0.018) [e]
					9	*63*	*3.9×10^{-1}*		(0.023) [e]

[a] M.A. El-Sayed, M.T. Wauk and G.W. Robinson, Mol. Phys. 5 (1962) 205.
[b] N. Hirota and C.A. Hutchison, J. Chem. Phys. 46 (1967) 1561; measurement in durene and durene-d_{14} at 77 K.
[c] R.J. Watts and S.J. Strickler, J. Chem. Phys. 49 (1968) 3867.
[d] T.D. Gierke, R.J. Watts and S.J. Strickler, J. Chem. Phys. 50 (1969) 5425. This value is an average of 3-methylpentane and ethanol solvent (glasses) values at 77 K.
[e] This is for percolation [6] *without* thermalization (see text).

(16), is indeed an order of magnitude smaller than the exciton lifetime τ_g, as expected from our derivation leading to eq. (18). While our calculated t may be off by a factor of ten (especially due to uncertainties in γ and $\bar{C}_S$), we have a "safety margin" of a factor of two-to-four in the t-column, i.e., before we expect a "quantum jump" of one $\bar{n}$ unit (say from 6 to 7 or vice versa). We can conclude that table 3 is at least a successful consistency test of our approach.

It should be noted that without the mathematical solution to the long-range percolation problem (fig. 7) we would not be able to perform the above test or even rationalize our data quantitatively. Fig. 7 is the necessary "dictionary" (mapping), relating the optimum superexchange range $\bar{n}$ with the critical percolation concentration $C_G(\bar{n})$, the only underlying assumption being that of a *square lattice* topology.

The justification or rationalization of an effective square topology upon which the calculations for the values of $C_G(\bar{n})$ were based is now discussed from the physical standpoint. Based on the experiments of Hanson [7] and of Hanson and Robinson [7], we know that the out-of-plane triplet exciton interactions are an order of magnitude smaller than the in-plane ($a\,b$) ones (a similar anisotropy is well known for anthracene [25]). This means that any superexchange "path" with *one* out-of-plane "step" is both less probable *and* more wasteful in time, by one order of magnitude! On the other hand, the gain in the geometrical factor $\Gamma_{\bar{n}}$ is relatively small, only on the order of 1 to 10 [30], the reason being that in the naphthalene crystal lattice there are *two* out-of-plane nearest neighbors of any given kind [say $\pm c$ or $\pm(c+a)$], compared to the *four* in-plane ones [$\pm\frac{1}{2}(a \pm b)$]. (Even if some out-of-plane interactions were nearly as large as the in-plane ones, the percolation concentration would only be reduced by about 1% (absolute) or less, based on a two-layer percolation calculation [6].) If a single translational neighbor interaction were to dominate [i.e., a "bond" along $a, b, c, (a+c)$, etc., crystallographic direction], and not the nearest neighbor, interchange equivalent interaction [$\frac{1}{2}(a+b)$], then the interaction topology would be *one-dimensional*, with no percolation phenomenon possible below $C_g \approx 1$. This is obviously not the case. Moreover, even for a $C_g \approx 1$ condition, independent energy transfer experiments for the first triplet exciton transfer, involving mostly exchange and not superexchange interactions,

indicate that the transfer is effectively two- to three-dimensional [26].

At temperatures much higher than 2 K, eq. (1) is no longer valid. Guest–host thermalization occurs at those higher temperatures, a process competing (or rather cooperating) with the exciton superexchange transfer. As the host band is now utilized directly for the energy transfer, our simple percolation model above breaks down. However, it breaks down with a definite qualitative result: The "effective" exciton percolation (including thermalization to the host band followed by direct transfer) is *more* efficient. At intermediate temperatures one expects a *lower* effective percolation concentration (compared to low temperatures), while at even higher temperatures there should be little concentration dependence, with all of the emission coming from the supertrap. A quantitative discussion, together with some pertinent experimental results, is reserved for a later paper. We would just point out here that system V (tables 2 and 3) is *already* in the "intermediate" temperature range even at 2 K, and these limiting cases will be discussed further, along with the above-mentioned higher temperature data. However, we note that the very low experimental effective percolation concentration (~0.001) is qualitatively consistent with that expected for "intermediate temperatures".

Finally, we would like to point out that our "low temperature" range of exciton percolation is bound on the high temperature side by eq. (1), and at the other extreme by

$$kT \gtrsim \beta . \tag{23}$$

Combining, we see:

$$E_h - E_g \gg kT \gtrsim \beta . \tag{24}$$

As β is [7] about 1.25 cm^{-1} and our lowest temperature is about 1.6 K, the conditional eq. (19) causes no problems. The reason for this limitation (eq. 19) is the requirement that guest pairs and/or clusters do not become supertraps for the guest (monomer) excitons. Thus, experiments much closer to 0 K would give results very different from ours. In fact, for the naphthalene singlet excitons, such cluster supertrapping effects are expected at 1.8 K ($\beta \approx 15$ cm^{-1}) [2], and have indeed been observed [9,26,28,29]. Essentially there one has an exciton cascade from guest monomers to dimers, trimers, etc., increasing with guest concentration almost until the static (effectively nearest neighbor) percolation concentration is reached, i.e., the limit where most discrete cluster energy levels merge into a quasicontinuous guest energy band [5]. Thus, the above cascade behaviour, coupled with dynamic exciton percolation (registered at the impurity supertrap) at about $C_G \approx 0.5$, is our predicted behaviour for the regime where

$$\beta \gg kT . \tag{25}$$

Because of the long triplet lifetime, i.e., to avoid significant dimer to monomer thermalization over a period of about 1 sec, the regime of eq. (25) is expected to hold only for temperatures about 0.1 K or lower (the "very low temperature limit").

Further, refined experiments are under way involving triplet lifetimes, delayed fluorescence and spatial measurements. Also planned is a computer simulation of the triplet exciton superexchange transfer, improving on some of our mathematical and physical approximations in the analytical derivations of the total transfer time. A discussion of supertrapping selectivity and its relation to weighted phonon densities [9] is also reserved for a separate paper, as is also the report on thermalization experiments and cooperative thermalization energy transfer.

9. Conclusions

(1) The specially developed mathematical model of "long range" percolation is found to be applicable to the naphthalene lowest triplet exciton in isotopic mixed crystals.

(2) The simple physical model of exciton superexchange (virtual band) is applicable to the trap–trap triplet exciton energy transfer in isotopic mixed naphthalene crystals at low temperature (2 K). These "energy conduction bands" narrow down to 10 hertz.

(3) The exciton transfer topology of $^3B_{1u}$ naphthalene is dominated by the ab plane, involving mainly the nearest neighbor (interchange equivalent) molecules. The exciton superexchange interactions are thus mostly two-dimensional and so is the exciton percolation. The interactions extend $\gtrsim$30 Å, encompassing $\gtrsim$100 sites.

(4) The "switching" of exciton triplet transfer in binary (isotopic mixed) naphthalene crystals at low

temperature (2 K) is determined, in a predictable way, by the concentration and energy denominator of the guest–host system, as well as the supertrap concentration. An impurity exciton "conduction" band may still be practically "open" at a 10 hertz bandwidth, but will be practically "closed" at a width of 1 hertz.

Note added in proof

The precision of the nearest neighbor interaction that we used (β) has just been significantly improved (to 1.25 ± 0.05 cm^{-1}) by B.J. Botter, C.J. Nonhof, J. Schmidt and J.H. Van der Waals [Chem. Phys. Lett. 43 (1976) 210]. This shows, by comparison with the Davydov splitting of the neat crystal [7], that the next-nearest *interchange-equivalent* pairwise interaction is *at least* one order of magnitude smaller, whether it is an in-plane one or an out-of-plane one [i.e., $\frac{1}{2}(a+b)+c$]. This is completely consistent with our model. However, it does not relate directly to the magnitude of the translationally-equivalent interactions.

We would also point out that the recently published paper by L. Altwegg, M. Chabr and I. Zschokke-Gränacher [Phys. Rev. B14 (1976) 1963] claims that the out-of-plane interactions in naphthalene are several orders of magnitude smaller than the in-plane ones. This is completely consistent with our findings.

Acknowledgement

We would like to thank Professor P.N. Prasad for very helpful discussions.

References

[1] M.A. El-Sayed, M.T. Wauk and G.W. Robinson, Mol. Phys. 5 (1962) 205;
G.C. Nieman and G.W. Robinson, J. Chem. Phys. 37 (1962) 2150;
G.W. Robinson and R.P. Frosh, J. Chem. Phys. 38 (1963) 1187;
H. Sternlicht, G.C. Nieman and G.W. Robinson, J. Chem. Phys. 38 (1963) 1326;
G.F. Hatch and G.C. Nieman, J. Chem. Phys. 48 (1968) 4116;
S.D. Colson and G.W. Robinson, J. Chem. Phys. 48 (1968) 2550.

[2] R. Kopelman, Rec. Chem. Progr. 31 (1970) 211;
H.-K. Hong and R. Kopelman, J. Chem. Phys. 55 (1971) 724.

[3] D.L. Dexter, J. Chem. Phys. 21 (1953) 836;
Th. Foerster, Annal. Phys. Ser. 6 Vol. 2, 55 (1948) 55. [English Translation (1974) by R.S. Knox, Univ. of Rochester, N.Y. 14627].

[4] R. Kopelman, E.M. Monberg, F.W. Ochs and P.N. Prasad, J. Chem. Phys. 62 (1975) 292;
R. Kopelman, in: Topics in Applied Physics, Vol. 15: Radiationless Processes in Molecules and Condensed Phases, ed. F.K. Fong (Springer, Berlin, 1976);
F.K. Fong (Springer, Berlin, 1976);
J. Hoshen and R. Kopelman, J. Chem. Phys. 65 (1976) 2817;
R. Kopelman, J. Phys. Chem. 80 (1976) 2191.

[5] H.-K. Hong and R. Kopelman, J. Chem. Phys. 55 (1971) 5380.

[6] J. Hoshen, E.M. Monberg and R. Kopelman, unpublished; see also
J. Hoshen and R. Kopelman, Phys. Rev. B 14 (1976) 3438.

[7] D.M. Hanson, J. Chem. Phys. 52 (1970) 3409;
D.M. Hanson and G.W. Robinson, J. Chem. Phys. 43 (1965) 4174;
T.L. Muchnik, R.E. Turner and S.D. Colson, Chem. Phys. Lett. 42 (1976) 570.

[8] C.L. Braun and H.C. Wolf, Chem. Phys. Lett. 9 (1971) 260.

[9] F.W. Ochs, Ph.D. Thesis, The University of Michigan (1974);
F.W. Ochs and R. Kopelman, Appl. Spectr. 30 (1976) 306.

[10] F.W. Ochs, P.N. Prasad and R. Kopelman, Chem. Phys. 6 (1974) 253.

[11] D.M. Hanson, J. Chem. Phys. 51 (1969) 5063.

[12] V.K.S. Shante and S. Kirkpatrick, Advan. Phys. 20 (1971) 325.

[13] R. Kopelman, in: Excited States, Vol. II, ed. E.C. Lim (Academic Press, New York, 1975) p. 33.

[14] A.I. Kitaigorodskii, Organic Chemical Crystallography (Consultants Bureau, New York, 1961).

[15] See second and third references of [4].

[16] E.W. Montroll and G.H. Weiss, J. Math. Phys. 6 (1965) 167;
E.W. Montroll, J. Math. Phys. 10 (1969) 753.

[17] R.P. Hemenger, R.M. Pearlstein and K. Lakatos-Lindenberg, J. Math. Phys. 13 (1972) 1056.

[18] This assumes a guest "superlattice" or coherent potential approximation [17], which is not completely justified for our guest concentrations (≤ 0.1). We plan to improve on eq. (7), using computer simulation for our binary system.

[19] The "largest path" is defined as the longest one "fast enough" to be competitive (see eqs. 13 and 17).

[20] This again is rough as the shorter (and longer) paths are not an insignificant fraction of the "largest" one. This point will also be checked quantitatively by computer simulation.

[21] Within a factor of four.
[22] They are rare due to the time restriction (see also [19]).
[23] F.W. Ochs, P.N. Prasad and R. Kopelman, unpublished.
[24] For the isotopic supertraps this appears reasonable, even though we detect some trapping selectively [9] (see text and figs. 1–4]. For BMN we assume the triplet case to be similar to the singlet case: R. Kopelman, E.M. Monberg, F.W. Ochs and P.N. Prasad, Phys. Rev. Lett. 34 (1975) 1506.
[25] R. Kopelman and J.C. Laufer, in: Electronic Density of States, ed. L.H. Bennet, National Bureau of Standards Special Publication No. 323 (U.S.G.P.O., Washington, D.C. 1971); and references therein.
[26] H.C. Wolf and H. Port, in: Molecular Spectroscopy of Dense Phases, Proc. 12th European Congr. on Mol. Spectrosc., Strassbourg, France (1975), eds. M. Grosmann, S.G. Elkomos and J. Ringeissen (Elsevier, New York, 1976).
[27] H.C. Wolf, J. Luminescence 12/13 (1976) 33.
[28] E.M. Monberg, F.W. Ochs and R. Kopelman, unpublished.
[29] P. Argyrakis, E.M. Monberg and R. Kopelman, Chem. Phys. Lett. 36 (1975) 349.
[30] The largest increase in $\Gamma_{\overline{n}}$ occurs in our case for the values of $\overline{n}=9$ or 10. We note that if $\beta^* = 0.1\beta$, where β^* is an out-of-plane interaction, then for $\overline{n}^*=10$ (including nine in-plane and one out-of-plane bonds) one gets $\overline{\Gamma}^*=9\overline{\Gamma}$ and thus effectively a "Perrin" disk including three layers (two square lattice diamonds with $S_{max}=9$). This would reduce the percolation concentration $C_G(n^*)$ by less than a factor of two. The same is true if β^* is a next-nearest in-plane interaction. For smaller $\overline{n}^*$, the effect of β^* is even less important.